

Efficient FEM Solvers for Incompressible Nonlinear Flow Models

Stefan Turek, Hogenrich Damanik, Jaroslav Hron and Abderrahim Ouazzi*

Institute of Applied Mathematics, TU Dortmund, Dortmund

**corresponding author: stefan.turek@math.tu-dortmund.de*

Abstract

We present special numerical techniques for non-Newtonian flows including non-isothermal, shear/pressure dependent and particularly viscoelastic effects which are based on the log-conformation reformulation (LCR), including Oldroyd-B and Giesekus-type fluids as prototypical models. We utilize a fully coupled monolithic finite element approach which treats the velocity, pressure, temperature and the logarithm of the conformation stress tensor simultaneously. As a consequence, fully implicit time stepping and even direct steady approaches are possible such that pseudo-time stepping with correspondingly small time step sizes, which typically depend by stability reasons on the spatial mesh size, can be avoided. Based on an accurate FEM discretization with consistent edge-oriented stabilization techniques for the convective operators, the corresponding nonlinear systems for velocity, pressure, temperature and conformation stress tensor are treated by a discrete Newton method, and local grid refinement is applied to reduce the computational efforts and to increase the accuracy. Then, a special geometrical multigrid solver with modified Vanka smoother is used for the resulting linear subproblems to maintain high accuracy and robustness, particularly w.r.t. different rheological behaviour but also regarding different problem sizes and type of nonlinearity. The presented methodology is analyzed for the well-known 'flow around cylinder' problem and other prototypical flow configurations of benchmarking character. Similar to other authors, simulation results for Oldroyd-B fluids can be obtained with the LCR approach for a wide range of Weissenberg (We) numbers. The merit of our approach is that we can obtain the discrete approximations by a direct steady approach with a numerical effort which is rather independent of the examined We numbers. Moreover, the same 'black box' techniques can be applied to Giesekus flow models which seem to lead to acceptable approximations for a much higher range of We numbers, hereby showing the same advantageous numerical convergence behaviour.

1 Introduction

We consider problems of non-Newtonian flow that satisfy the momentum and continuity equation. The set of equations is written in terms of the Boussinesq approximation as follows

$$(VT) \begin{cases} \frac{\partial \mathbf{u}}{\partial t} + (\mathbf{u} \cdot \nabla) \mathbf{u} = -\nabla p + \nabla \cdot \mathbf{T} \\ \nabla \cdot \mathbf{u} = 0 \\ \frac{\partial \theta}{\partial t} + (\mathbf{u} \cdot \nabla) \theta = k_1 \Delta \theta + k_2 \mathbf{D} : \mathbf{D} \end{cases} \quad (1)$$

with the constitutive law $\mathbf{T} = 2\eta_s(\dot{\gamma}, \theta, p)\mathbf{D}$, shear rate $\dot{\gamma} = \sqrt{\text{tr } \mathbf{D}^2}$, symmetric velocity gradient $\mathbf{D} = \frac{1}{2}(\nabla \mathbf{u} + \nabla \mathbf{u}^T)$, and additional viscous dissipation term $\mathbf{D} : \mathbf{D}$. Here, k_1 and k_2 are the thermal diffusivity and viscous dissipation parameters. The fluid viscosity function will lead later to the power law and Cross model. Now, we call it velocity-temperature-pressure problem (VT). Furthermore, complex fluid flow problems in the area of viscoelasticity are also considered and are written in the following LCR formulation

$$(VS) \begin{cases} \frac{\partial \mathbf{u}}{\partial t} + (\mathbf{u} \cdot \nabla) \mathbf{u} = -\nabla p + \eta_s \Delta \mathbf{u} + \frac{\eta_p}{\Lambda} \nabla \cdot \mathbf{e} \boldsymbol{\psi} \\ \nabla \cdot \mathbf{u} = 0 \\ \frac{\partial \boldsymbol{\psi}}{\partial t} + (\mathbf{u} \cdot \nabla) \boldsymbol{\psi} - (\boldsymbol{\Omega} \boldsymbol{\psi} - \boldsymbol{\psi} \boldsymbol{\Omega}) - 2\mathbf{B} = \frac{1}{\Lambda} (e^{-\psi} - I) - \alpha e^{\psi} (e^{-\psi} - I)^2 \end{cases} \quad (2)$$

where $\boldsymbol{\psi}$, Λ are the LCR tensor and the relaxation time of the polymer. The parameter α is the Giesekus mobility factor which yields to the Oldroyd-B model if it is set to zero. Numerically, the relaxation time describes the complexity of the corresponding flow model which is commonly represented by the non-dimensional Weissenberg number $We = \Lambda \frac{u_c}{l_c}$ where u_c and l_c are just characteristic velocity and length. The total stress now consists of viscous and elastic parts as well as the corresponding viscosities, η_s, η_p . The ratio $\beta = \frac{\eta_s}{\eta_p}$ denotes the viscous contribution to the total stress. We call this velocity-stress-pressure problem (VS).

2 FEM Discretization

The choice of FEM spaces for the Stokes problem is subject to the well-known compatibility condition between the velocity and pressure space, the so-called *inf - sup* condition named after Ladyzhenskaya, Babuška and Brezzi (LBB) [3]. Similarly, the addition of the weak form of the constitutive equation imposes a further compatibility constraint onto the choice of the approximations spaces of the velocity-pressure-stress. We choose the finite element pair Q_2P_1 which is popular for Stokes-like problems.

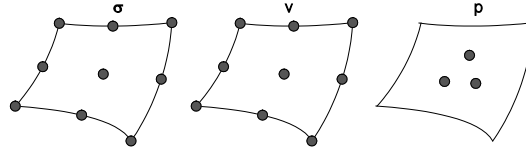


Figure 1: The finite element pair Q_2P_1

Bonito and Burman [4] have shown that inf-sup stability as well as stability for convection-dominated flows can be obtained by adding a consistent stabilization term penalizing the jump of the solution gradient over element edges E , see also [7]. The same technique can be utilized in the equations for the stress tensor (or for the logarithm of the conformation stress in the case of LCR), particularly for relaxing the choice of the stress space in the absence of a pure viscous contribution. Moreover, since the convective terms of the constitutive equations also require appropriate stabilization techniques, the corresponding edge-oriented jump terms for the stress have been introduced which read as follows

$$J_\sigma = \sum_{edge \ E} \gamma h_E^2 \int_E [\nabla\psi]:[\nabla\chi] \, ds. \quad (3)$$

We end up with the same type of nonlinear saddle point problems for any set of equations mentioned before, namely

$$\begin{pmatrix} A & B^T \\ B & 0 \end{pmatrix} \begin{pmatrix} \tilde{\mathbf{u}} \\ p \end{pmatrix} = \begin{pmatrix} rhs \ \tilde{\mathbf{u}} \\ rhs \ p \end{pmatrix} \quad (4)$$

where $\tilde{\mathbf{u}}$ may consist of the coefficient vector representing the velocity, temperature (VT) and conformation/LCR tensor (VS). Here, A includes all convection and diffusion operators, including the above additional stabilization terms, J_σ , of edge-oriented type (EOFEM).

2 Solvers

The Newton method is utilized for the linearization of the system. We start with a system for the residual of the nonlinear algebraic equations and treat them in a monolithic way

$$\mathcal{R}(\mathbf{x}) = 0 \quad (5)$$

where \mathbf{x} represents the vector of the coefficients corresponding to all physical unknowns. Note, the level set equation is treated separately. We apply the Newton method with damping which results in iterations of the form

$$\mathbf{x}^{n+1} = \mathbf{x}^n + \omega^n \left[\frac{\partial \mathcal{R}(\mathbf{x}^n)}{\partial \mathbf{x}} \right]^{-1} \mathcal{R}(\mathbf{x}^n). \quad (6)$$

It is evident that the Newton method needs to compute the first derivative of the residual with respect to the current solution vector (sometimes it is called tangent stiffness matrix) at every Newton step and level. This can be done analytically, by means of taking the Fréchet derivative of the nonlinear operator, or by using divided difference techniques

$$\left[\frac{\partial \mathcal{R}(\mathbf{x}^n)}{\partial \mathbf{x}} \right]_{ij} \approx \frac{\mathcal{R}_i(\mathbf{x}^n + \varepsilon \mathbf{e}_j) - \mathcal{R}_i(\mathbf{x}^n - \varepsilon \mathbf{e}_j)}{2\varepsilon} \quad (7)$$

where the vector \mathbf{e}_j is the unit vector of j direction. On this study, we use the latter approach where the parameter is set to be constant, i.e. $\varepsilon = \sqrt{DBL_Machine}$. The structure of the Jacobian matrix depends on the physical unknowns. For (VT) problems with $\tilde{\mathbf{u}} = (u, \theta)$, (VS) problem with $\tilde{\mathbf{u}} = (u, \tau)$, and even mixed problems of both we obtain

$$\begin{bmatrix} A_u & \tilde{H}_u^T \\ H^u & A_\theta \end{bmatrix}, \quad \begin{bmatrix} A_u & C^T \\ \tilde{C} & A_\tau \end{bmatrix}, \quad \begin{bmatrix} A_u & C^T & \tilde{H}_u^T \\ \tilde{C} & A_\tau & 0 \\ H^u & 0 & A_\theta \end{bmatrix}. \quad (8)$$

Here, H^u corresponds to the bilinear forms of the viscous dissipation terms and C^T corresponds to the bilinear form of viscoelastic dissipation terms.

We use the concept of the local PSC approach which is to solve ‘**exactly**’ on fixed patches and to perform an outer Gauß-Seidel-like iteration. This approach can be interpreted as generalization of block-Jacobi/Gauß-Seidel methods for saddle point problems which contains modifications of classical schemes like the Vanka smoother [18]. The idea of the local PSC smoother is to apply a defect correction of the type

$$\mathbf{x}_{j+1} \leftarrow \mathbf{x}_j + \omega \mathbf{C}^{-1}(\mathbf{b} - \mathbf{A}\mathbf{x}_j), \quad \omega > 0 \quad (8)$$

element by element, with \mathbf{C} an appropriate preconditioner. The underlying mesh of the finite element space on level h is denoted by Ω_h . In an outer loop over all elements $\mathbf{K} \in \Omega_h$, a global defect $\mathbf{r}_j = (\mathbf{b} - \mathbf{A}\mathbf{x}_j)$ is built. The components of the defect which do not belong to the current element are forced to zero. As a consequence, the global defect can be reduced to a local defect r_j^K , and the global preconditioner reduces to a local preconditioner as all rows and columns which do not belong to that element can be eliminated. This gives a local linear system and a local update for the current element. A more formal description reads as follows (Algorithm):

Algorithm: Smoothing steps

Input: predefined constant: $\omega > 0$, Number of smoothing steps: NSM

For $j=1$ to NSM do

 For $\mathbf{K} \in \Omega_h$ do

$$x_{I(k)} \leftarrow x_{I(k)} + \omega \mathbf{C}_k^{-1}(\mathbf{b} - \mathbf{A}\mathbf{x})_{I(k)}$$

Return \mathbf{x}

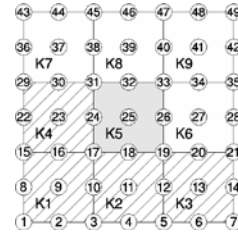


Figure 2: The smooting illustration

Let $I(k)$ identify a list of all degrees of freedom which are located on element \mathbf{K} . It contains the numbers for the velocity and pressure components, as well as temperature and stress in the case of (VT) and (VS) problems. Hence, $A_{I(k)}$ denotes a quadratic matrix which corresponds to the rows and columns of \mathbf{A} restricted by the index set $I(k)$. In the same way, $x_{I(k)}$, $b_{I(k)}$ and $r_{I(k)} = (\mathbf{b} - \mathbf{A}\mathbf{x})_{I(k)}$ refer to the subvectors of \mathbf{x} , \mathbf{b} and \mathbf{r} restricted to element \mathbf{K} . Having $A_{I(k)}$, $x_{I(k)}$ and $b_{I(k)}$ localized, one may obtain the preconditioner \mathbf{C}_k^{-1} by invoking a LU decomposition (e.g. with the LAPACK package) of the (small) matrix $A_{I(k)}$. Finally, a constant damping parameter, ω , is introduced and the corresponding components of $x_{I(k)}$ are updated. An illustration of the smoothing process is shown by Fig. 2 in which the elements $\mathbf{K}_1, \dots, \mathbf{K}_4$ are already processed. On the next element \mathbf{K}_5 the degrees of freedom with the components 17, 18, 19, 24, 31 will be updated again due to the Gauß-Seidel character while the components 25, 26, 32, 33 will be computed for the first time. The size of \mathbf{C}_k^{-1} depends on the problem, i.e., for (VT) and (VS) it has a size of 30×30 and 48×48 respectively when using the $\mathbf{Q}_2\mathbf{P}_1$ FEM approach. In order to demonstrate the solver flexibility with respect to different flow problems, an ‘F-cycle’ of multigrid is used with 4 smoothing steps in the following numerical tests.

3 Numerical experiments

We apply the above numerical methods to the flow around cylinder configuration, Fig. 3, and solve (VS) flow equations with nearly 3 million unknowns for the finest level 5. The solver behaves very stable with respect to mesh refinement, Tab. 1, and it needs only few iterations to converge which is rather independent of the two viscoelastic models being used. Tab. 1 shows that the solution of $We=0.2$ converges to a mesh independent result of drag/lift.

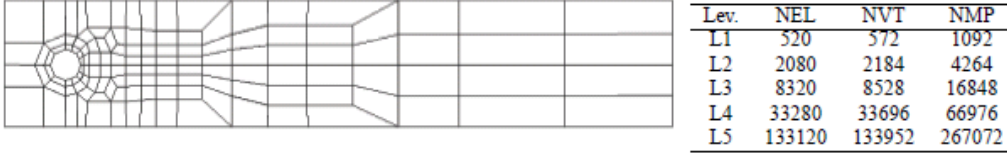


Figure 3: The finite element coarse mesh of flow around cylinder benchmark

Table 1: Flow around cylinder of Oldroyd-B (left)/Giesekus (right) model of $We=0.2$

Level	Drag/lift	NL/LL	Drag/lift	NL/LL
1	5.84074/0.00404	14/2	4.93283/ -0.00036	9/2
2	5.89550/0.00358	4/2	4.98376/ 0.00464	4/2
3	5.90790/0.00432	3/2	4.98415/ 0.00507	3/2
4	5.89463/0.00510	3/2	4.98230/ 0.00523	3/3
5	5.87765/0.00576	3/3	4.98286/ 0.00524	2/2

Furthermore, we apply the same problem to another configuration of planar flow around cylinder which is used to benchmark viscoelastic flow results, Fig. 3. A local refinement technique with hanging nodes is applied to the cylinder region and in the wake to reduce the computational effort at finest mesh. The Giesekus model is considered because it provides higher Weissenberg number simulation (here up to $We=100$) without showing any problem on how the numerical method behaves with respect to higher nonlinearity, Tab. 2. The benefit of the proposed method is that one does not need to use a nonsteady approach which is clearly very time consuming. Few nonlinear steps are needed to march from lower up to the expected higher We number.

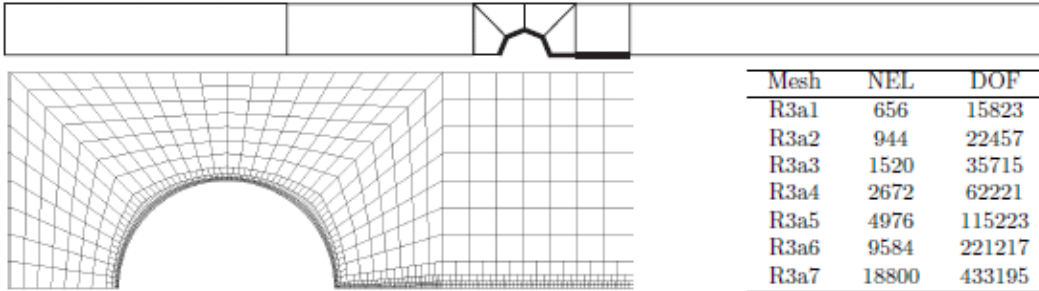


Figure 3: The finite element coarse mesh of planar flow around cylinder with local refinement

Table 2: Flow around cylinder for the Giesekus model up to $We=100$

We	Drag	Peak stress	NL	We	Drag	Peak stress	NL
30	88.304	6318.79	5	70	85.356	13773.61	4
40	87.256	8311.32	5	80	84.937	15502.45	4
50	86.476	10199.1	4	90	84.585	17207.87	4
60	85.859	12010.57	4	100	84.287	18897.95	4

4 Summary

We have shown efficient FEM numerical methods for nonlinear fluids which can be applied to any complex fluid flow problems, (VT) or (VS) or even mixed problems of both. The discretization in space is based on the LBB-stable Q_2P_1 finite element approach to maintain highly accurate solutions while the resulting discrete systems are solved iteratively. The core technique of the method is the monolithic treatment of all physical unknowns for both linear and nonlinear solvers. In the linear solver, a multigrid iteration is used with the help of robust Vanka smoother. For the nonlinear solver, a finite difference approximation of the related Jacobian matrix is used which serves as “black-box” for any complex fluid flows. We observe an excellent convergence behavior for solving such complex flow models irrespective of mesh refinement and fluid models being used. In future research, we plan to show that the same method can be applied to multiphase flow phenomena [5,6].

5 References

- [1] Damanik, H.; Hron, J.; Ouazzi, A.; Turek, S.: Monolithic Newton-multigrid solution techniques for incompressible nonlinear flow models, *Int. J. Numer. Meth. Fluids*, accepted, 2012.
- [2] Damanik, H.; Hron, J.; Ouazzi, A.; Turek, S.: A monolithic FEM approach for the log-conformation reformulation (LCR) of viscoelastic flow problems, *J. Non-Newtonian Fluid Mech.*, 19-20, 165, 1105-1113, 2010.
- [3] Girault, V, Raviart, P A. *Finite Element Methods for Navier-Stokes equations*. Springer, 1986. Berlin-Heidelberg.
- [4] Bonito, A. and Burman, E. A continuous interior penalty method for viscoelastic flows. *Siam Journal of Scientific Computing*, 30:1156–1177, 2008.
- [5] Münster, R.; Mierka, O.; Turek, S.: Finite Element fictitious boundary methods (FEM-FBM) for 3D particulate flow, *Int. J. Numer. Meth. Fluids*, accepted, 2011.
- [6] Turek, S.; Mierka, O.; Hysing, S.; Kuzmin, D.: Numerical study of a high order 3D FEM-Level Set approach for immiscible flow simulation, P. Neittaanmäki’s 60th jubilee publication, Wiley-VCH, accepted, 2012.
- [7] Turek, S.; Ouazzi, A.: Unified edge-oriented stabilization of nonconforming FEM for incompressible flow problems: Numerical investigation. *J. Numer. Math.* 2007; 15:299-322.